

Preparation and photocatalytic characteristic of Sb-doped anatase TiO₂ powders

Z. CHEN, Z. ZHANG^a, Z. ZHONG^a, C. ZHANG^a, J. XU*

School of Nuclear Science and Technology, Lanzhou University, Lanzhou 730000, PR China

^aLaboratory for Quantum Engineering and Micro-Nano Energy Technology and Department of Physics, Xiangtan University, Xiangtan 411105, PR China

Sb-doped nano titanium dioxide powders were prepared by hydrothermal method. Samples were then characterized using SEM or XRD. The results indicated that all samples were anatase phase TiO₂ and the particle sizes were all under 10nm. The DRS experiments showed that light absorption was improved when the Sb³⁺ was doped properly. Moreover, we discussed about the red-shift of DRS and brought forward luminescence mechanistic of TiO₂ with Sb-doping according to the fluorescence emission spectra. At last, the photocatalytic degradation of methyl orange was tested for all samples, and the photocatalytic efficiency was greatly enhanced when the 0.5% Sb³⁺ was doped.

(Received March 17, 2011; accepted April 11, 2011)

Keywords: Nano titanium dioxide, Sb-doped, Fluorescence emission spectra, Photocatalysis, Methyl orange

1. Introduction

Since Fujishima and Honda had reported that water can be decomposed into hydrogen and oxygen using TiO₂ electrode in 1972 [1], lots of attention has been paid on their possible applications in photocatalysis especially [2-3]. Although the anatase TiO₂ has better photocatalytic and photoelectric activity, the application is limited due to the large band gap (3.2eV for anatase) and high recombination rate of electron-hole pairs in TiO₂. During the past decades, many researchers had been focused on the modification of nano TiO₂ to solve this problems, such as surface photosensitization [4] and ion doping [5-8]. The absorption of visible light was enhanced and the photocatalytic degradation of organic pollutants performed well when the TiO₂ was modified appropriately [9]. Therefore, TiO₂ can be used as the anode in dye-sensitized solar cells, the sunscreen in some cosmetics and the photocatalytic in decomposition after modification.

Both the fluorescence emission spectrum and the diffuse reflectance spectrum have much to do with the bandgap structure of ion-doped TiO₂, but little research has been done in the mechanism of the two spectra simultaneously. Also, whether Sb-doping can improve the photocatalytic activity of TiO₂ was still controversial. Castro et al. [5] showed that the photocatalytic efficiency of Sb-doped TiO₂ was improved significantly. However, Choi et al. [10] reported that dopant with a closed-shell electronic configuration, such as Sb⁵⁺, has little effect in increasing its photoreactivity. Besides, the methods of preparing Sb-doped TiO₂ and the pH in the process also influenced the photoreactivity of dye [11-13]. So the

mechanism and factors influencing the photocatalytic efficiency of Sb-doped TiO₂ are still unclear.

In this study, the ultra-fine Sb-doped nano anatase TiO₂ powders were prepared by hydrothermal method, without calcinations in the oven compared to traditional methods [14-15]. The enhancement in absorption to visible light and the split of fluorescence emission peak for all Sb-doped samples were discussed according to the bandgap theory. Moreover, the influence of Sb concentration and the corresponding photocatalytic degradation of methyl orange were investigated in details. For the Sb-doped samples, the absorption to visible light and the degradation activity on methyl orange were improved significantly compare with pure nano TiO₂.

2. Experimental

2.1 Material synthesis

All reagents used in the experiments were purchased from commercial sources in China as received. The materials used included titanic chloride (TiCl₄, CP), absolute alcohol (C₂H₅OH, AR), propanetriol (C₃H₈O₃) and antimonous chloride absolute alcohol solution (SbCl₃, 0.01 mol/L). The propanetriol (0.44 ml, 6 mmol) and the titanic chloride (2.035 ml, 6 mmol) were added to the absolute alcohol firstly. The antimonous chloride absolute alcohol solution was then added to the mixture by the mole ratio of 0.0%, 0.3% (1.8 ml), 0.5% (3 ml), 0.7% (4.2 ml) and 0.9% (5.4 ml) respectively. The whole volume was held at 20 ml at last and the stirring was underway in the process above. The solution was then

sealed off by the autoclave and was kept 16 hours at 120 °C. The obtained white samples were centrifuged by absolute alcohol and dried at 60 °C for 3 hours finally.

2.2 Characterization

The morphology of the samples was investigated using Hitachi S-4800 field-emission scanning electron microscopy. The phase identification of samples was carried out by a Rigaku D/Max-2400 X-ray diffractometer with Cu K α radiation. Diffuse reflectance spectra (DRS) of samples were collected on finely ground samples by an UV-vis spectrophotometer (PE lambda950) using BaSO₄ as a reference. The fluorescence emission spectra were obtained by a FLS-920T fluorescence spectrophotometer equipped with Xe 900 (450W xenon arc lamp) as the light source with spectral slits width of 0.5 nm.

2.3 Evaluation of the photocatalysis

Methyl orange and micron-sized commercial TiO₂ were purchased in China without further purification, and the methyl orange was chosen to be the target compound to degrade. In this experiment, 3 mg methyl orange (AR) was added to 90 ml distilled water firstly, 90 mg commercial TiO₂ (CP) and samples were then dispersed into the methyl orange solution in the dark after 8 min sonic oscillation respectively. The 20 min stirring was then in the process to establish an adsorption-desorption equilibrium. The 90 min ultraviolet irradiation was carried out by ZF-I ultraviolet analytic instrument and the 254 nm was chosen as the wavelength (the solution was magnetically stirred throughout the process). At last, the UV-Vis absorption spectra of the solution were measured under UV-vis spectrophotometer (Shimadzu UV-2550) after centrifugal separation.

3. Results and discussion

3.1 SEM images and XRD analysis

The SEM images of the pure and Sb-doped samples are shown in Fig. 1. The particle sizes of nano TiO₂ powders are small and have not much difference after Sb-doping. From the picture, the nano particles were aggregated in large area probably because of large surface energy and activity in nano TiO₂. Fig. 2 shows XRD patterns of the Sb-doped TiO₂ powders with the Sb-ion concentration 0.0%, 0.3%, 0.5%, 0.7% and 0.9%. Through comparison with the JCPDS, only peaks corresponding to the anatase TiO₂ phase were observed for all the samples. The sizes of all particles are under 10nm in average after analyzing XRD by Jade 5.0 software. Moreover, the <101> peaks of all Sb-doping samples shift to a low angle obviously compared to the pure TiO₂ in Fig. 2, which indicates that larger Sb³⁺ have

entered into the anatase structure and substituted for Ti⁴⁺ sites in TiO₂ lattice successfully. A similar result has been shown for Co-doped TiO₂ thin films [16]. However, the shift of <101> peak is not in line with the Sb concentration because Sb³⁺ is easily oxidized to Sb⁵⁺ in the autoclave with oxidizing atmosphere.

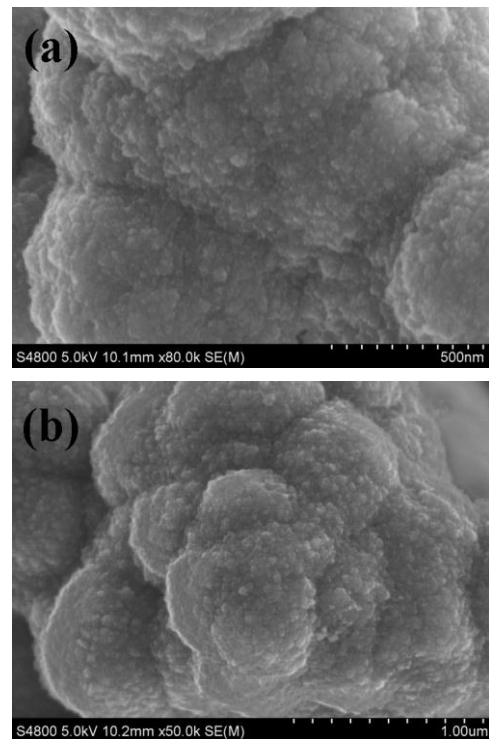


Fig. 1. (a) SEM image of undoped nanoscale TiO₂ powders. (b) SEM image of 0.5% Sb-doped nanoscale TiO₂ powders.

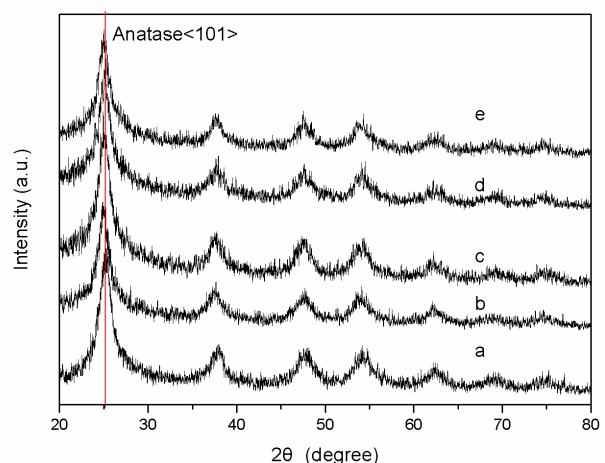


Fig. 2. XRD patterns of pure and Sb-doped TiO₂ powders according to different concentration, showing a single phase anatase structure and no impurity peak. (a) 0.0% (b) 0.3% (c) 0.5% (d) 0.7% (e) 0.9%.

3.2 UV-Vis diffuse reflectance spectra

To investigate whether the absorption to visible light was extended after Sb-doping, the diffuse reflectance spectra (DRS) of pure and 0.9% Sb-doped TiO_2 were presented in Fig. 3. Also, the rest spectra of Sb-doping were between a and b. The result indicates that the absorption intensity varies little after Sb-doping compared with the pure absorption value. The spectrum of sample with 0.9% Sb-doping has the largest red-shift extent and the best absorption intensity in contrast with other samples. According to the band theory, Sb^{5+} which is oxidized from Sb^{3+} has the similar radius with Ti^{4+} , so the donor level can be mainly made up in the forbidden band of TiO_2 when Sb^{3+} is doped, and the donor level is closed to conduction band. Not only excitation electrons from valence band can jump into donor level, the electron can jump into conduction band from donor level when the appropriate photons are absorbed. It means that the absorbable visible light is extended after Sb-doping because of the lesser distance and energy between the donor level and the conduction band, so the red-shift appears in the DRS of Sb-doped TiO_2 . As we know, ultraviolet radiation can be divided into UV-A (320-400 nm), UV-B (280-320 nm) and UV-C (190-280 nm) areas according to the wavelength. The red-shift of the DRS clearly indicates that the TiO_2 can screen ultraviolet radiation of UV-A area effectively after Sb-doping, so the doped samples can be industrially used in the sunscreens and other cosmetics.

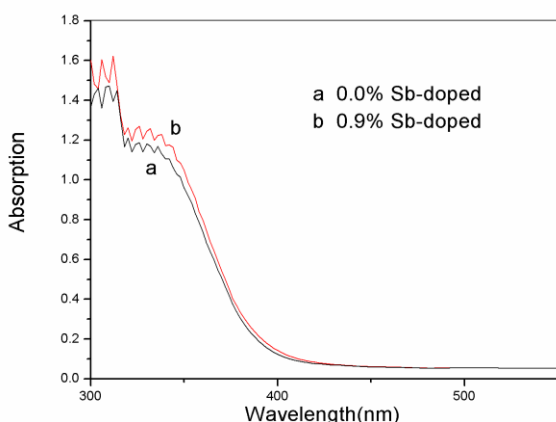


Fig. 3. Diffuse reflection spectra of hydrothermally synthesized Sb-doped samples: (a) undoped TiO_2 (b) 0.9% Sb-doped TiO_2 .

3.3 Fluorescence emission spectra

For a further analysis of the bandgap structure and the relationship to DRS, the fluorescence emission spectra of all the samples were performed, in which the wavelength ranging from 450 nm to 550 nm is

considered and the excitation wavelength is 329 nm, the results are given in Fig. 4. From the figure, it can be seen that there is better luminescence at 489 nm for all samples, but the peaks have split and one of the splitting peaks is located at 491 nm for all Sb-doped samples. We consider the peaks at 489 nm are caused by excitons. Firstly, the electron jumps from valence band to conduction band when it is excited, and the relative hole is produced in the valence band, the hole and the electron then form the bound electron hole pair due to coulombic force, which is so-called exciton and its energy is less than the forbidden gap. The energy can be released when a pair of exciton encounters. Moreover, the peak of 489 nm is correlated with the released energy as we considered in Fig. 3. The reason for the peak splitting after Sb-doping is discussed according to the existence of donor level which is obtained from the red-shift of DRS. In the Sb-doped samples, the electron can jump from valence band to donor level when it is excited, so the hole leaves in the valence band and this type of exciton is made up. The energy of this exciton is less than the exciton's which we consider before, and the location of the peak will be larger when the relative energy is released. That is the reason for the peak splitting after Sb-doping.

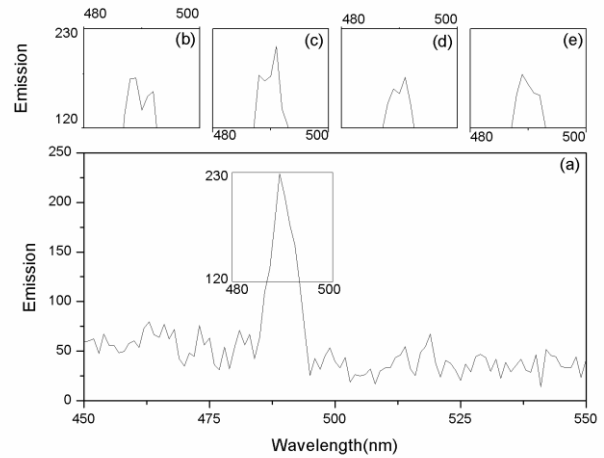


Fig. 4. Fluorescence emission spectra ranging from 450 nm to 550 nm for all samples with different Sb concentrations. (a) 0.0% (b) 0.3% (c) 0.5% (d) 0.7% (e) 0.9%.

3.4 UV-Vis absorption spectra and photocatalytic results

The photocatalytic efficiency on methyl orange solution of pure and 0.5% Sb-doped TiO_2 were tested followed by 90 min UV irradiation, and the commercial TiO_2 was included for a comparative purpose. Fig. 5 shows UV-Vis absorption spectra of methyl orange solution without the sample (a), with commercial TiO_2 (b), pure TiO_2 (c) and 0.5% Sb-doped TiO_2 (d)

respectively, the rest spectra of Sb-doping were between c and d. There was no participation of distilled water in the process of preparing samples, and all the samples were washed by absolute ethyl alcohol in the centrifugal separation, so the residual ethyl alcohol left on the surface of samples, the solvent content of methyl orange solution is then changed after adding the samples in and the UV-Vis absorption spectra display the red-shift compared with curve a and b. But it is the red-shift that the samples can be as a better photocatalyst because of more reasonable visible light using. According to the photocatalytic efficiency formula:

$D = (A_0 - A) / A_0 \times 100\%$ (The original absorption value of methyl orange solution is A_0 , and A is for current value), the photocatalytic effect is the best when the spectrum is at the lowest in Fig. 5. The results indicate that all the samples have the better photocatalytic activity compared with commercial TiO₂ and the activity is the best when the 0.5% Sb³⁺ is doped.

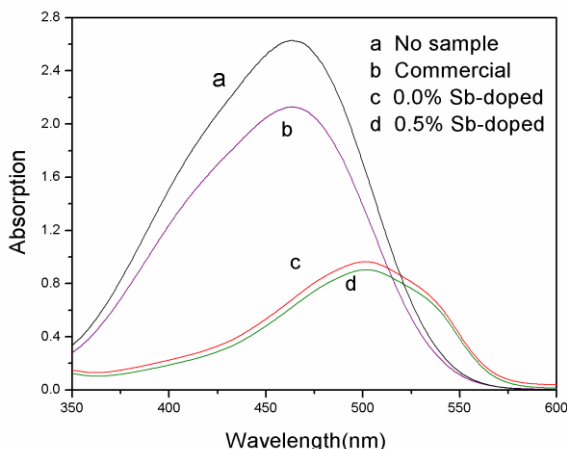
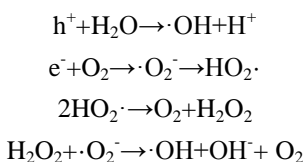


Fig. 5. UV-Vis absorption spectra of methyl orange solution after 90min under UV irradiation. (a) solution without sample, (b) solution with commercial TiO₂, (c) solution with undoped sample, (d) solution with 0.5% Sb-doped sample.

As we know, the mechanistic of photocatalysis is that many holes (h^+) and electrons (e^-) would be produced under the irradiation of UV-light, and the water would be oxidized under the action of h^+ , on the contrary, the oxygen would experience the process of reduction by e^- . The chemical reaction of this process is as follows:



The organics can be oxidized and decomposed into

carbon dioxide and water finally because the group of $\cdot OH$ has the good ability of oxidation. According to the analysis in XRD, the larger Sb-ion has entered into the anatase structure and substituted for Ti cations sites in TiO₂ lattice, the lattice will be expanded due to the interaction of the Sb cations. Further more, the lattice distortional strain energy and the strain energy will be existed from the lattice expansion, therefore the oxygen atom on the surface of TiO₂ will escape from the lattice as a kind of hole capture for compensating the lattice stress, and the speed of recombination will be let down between photoinduced electrons and holes. At the same time, more electrons will be excited into conduction band under UV irradiation, so more electron hole pairs will be produced, and photocatalytic efficiency will be enhanced. One the other hand, according to the research by Fox [17], the photoinduced electrons can be separated validly when the light penetrates the solid and then enters into the thickness of space charge layer. The thickness of space charge layer gets narrow and the intensity of electric field increases in line with the proportion of Sb-doping, which is the reason why the electron hole pairs can be separated in this area. We consider the space charge layer get very narrow and the light have passed through the layer when the Sb-ion concentration exceeds 0.5%, so the speed of recombination for photoinduced electrons and holes will be increased, and the photocatalytic efficiency get lower again.

The fluorescence emission spectra of nano TiO₂ were caused by recommendation between electrons and holes according to Suisalu [18]. Moreover, the photocatalytic effect was significantly influenced by the rate of recommendation. Whether there is matching between the strength of fluorescence emission spectra and the photocatalytic properties of nano TiO₂, many research hold different views [19-20]. In this paper, the photocatalytic activity is the best and the peak of 491nm is the highest from fluorescence emission spectra when the 0.5% Sb is doped. But the further study on this relationship and mechanism is necessary.

4. Conclusions

In conclusion, Sb-doped anatase TiO₂ powders were synthesized successfully by hydrothermal method. There was no calcination in the preparing process, and the low temperature was needed. The absorption of the sample with 0.9% Sb-doping behaved best according to the DRS. Also, we discussed the red-shift of DRS and brought forward luminescence mechanistic of Sb-doped TiO₂ according to the fluorescence emission spectra. Moreover, the UV-Vis absorption spectra were analyzed, and the results indicated that the 0.5% Sb-doped TiO₂ had the best photocatalytic activity on the methyl orange solution.

Acknowledgements

The author sincerely acknowledges the photocatalytic measurement support by the Gansu Academy of Science. The author is also thankful the financial support of this work by the National Science Foundation of China (Grant Nos. 10374039, 10274088).

References

- [1] A. Fujishima, Nature, **238**, 37 (1972).
- [2] A. Danion, J. Disdier, C. Guillard, N. Jaffrezic-Renault, Journal of Photochemistry and Photobiology A: Chemistry, **190**, 135 (2007).
- [3] M. Anpo, M. Takeuchi, Journal of Catalysis, **216**, 505 (2003).
- [4] B. O'regan, M. Grä tzel, (1991).
- [5] A. Castro, M. Nunes, M. Carvalho, L. Ferreira, J. Jumas, F. Costa, M. Florêncio, Journal of Solid State Chemistry, **182**, 1838 (2009).
- [6] L. Ren, F. Yang, Y. Zhang, J. Yang, M. Li, Chinese Journal of Inorganic Chemistry, **24**, 541 (2008).
- [7] Y. Bessekhouad, D. Robert, J. Weber, N. Chaoui, Journal of Photochemistry and Photobiology A: Chemistry, **167**, 49 (2004).
- [8] R. Asahi, T. Morikawa, T. Ohwaki, K. Aoki, Y. Taga, Science, **293**, 269 (2001).
- [9] Y. Liu, C. Liu, J. Wei, R. Xiong, C. Pan, J. Shi, Applied Surface Science, (2010).
- [10] W. Choi, A. Termin, M. Hoffmann, The Journal of Physical Chemistry, **98**, 13669 (1994).
- [11] D. Mardare, G. Rusu, Materials Science and Engineering B, **75**, 68 (2000).
- [12] C. Chen, C. Lu, F. Mai, C. Weng, Journal of hazardous materials, **137**, 1600 (2006).
- [13] M. Qamar, Desalination, (2010).
- [14] M. Abdullah, F. Chong, Journal of hazardous materials, **176**, 451 (2010).
- [15] D. Ren, Z. Zhang, Chinese Journal of Chemical Physics, **19**, 549 (2006).
- [16] M. Cui, J. Zhu, X. Zhong, Y. Zhao, X. Duan, Applied Physics Letters, **85**, 1698 (2004).
- [17] M. Fox, M. Dulay, Heterogeneous photocatalysis, Name: Chemical Reviews.
- [18] A. Suisalu, J. Aarik, H. Mändar, I. Sildos, Thin Solid Films, **336**, 295 (1998).
- [19] F. Li, X. Li, X. Li, H. Wan, Acta Chimica Sinica-Chinese Edition-, **59**, 1072 (2001).
- [20] S. Fengyu, W. Ming, L. Wenzhao, L. Xinyong, G. Wanzhen, W. Fudong, Chinese journal of catalysis, **19**, 121 (1998).

* Corresponding author: jinzhangxu.lzu@gmail.com